9-29-2004

Single-sided CZT strip detectors

John R. Macri
University of New Hampshire - Main Campus, John.Macri@unh.edu

B Donmez
University of New Hampshire - Main Campus

Mark Widholm
University of New Hampshire - Main Campus, Mark.Widholm@unh.edu

L A. Hamel
University of Montreal

Manuel Julien
University of Montreal

See next page for additional authors

Recommended Citation

John R. Macri ; Burcin Donmez ; Mark Widholm ; Louis-Andre Hamel ; Manuel Julien ; Tomohiko Narita ; James M. Ryan and Mark L. McConnell "Single-sided CZT strip detectors", Proc. SPIE 5501, High-Energy Detectors in Astronomy, 208 (September 29, 2004); doi:10.1117/12.551958; http://dx.doi.org/10.1117/12.551958

Authors

John R. Macri, B Donmez, Mark Widholm, L A. Hamel, Manuel Julien, T Narita, James M. Ryan, and Mark
L. McConnell

Single-sided CZT strip detectors

John R. Macri[*a], Burcin Dönmez[a], Mark Widholm[a], Louis-Andre Hamel[b], Manuel Julien[b],
Tomohiko Narita[c], James M. Ryan[a], Mark L. McConnell[a]

[a]Space Science Center, University of New Hampshire, 39 College Road, Durham, NH USA 03824
[b]Dept. of Physics, Univ. of Montreal, Chemin des Services, Montreal, Quebec, Canada H3T 1J4.
[c]Dept. of Physics, College of the Holy Cross, 1 College Street, Worcester, MA USA 01610

ABSTRACT

We report progress in the study of thick CZT strip detectors for 3-d imaging and spectroscopy and discuss two approaches to device design. We present the spectroscopic, imaging, detection efficiency and response uniformity performance of prototype devices. Unlike double-sided strip detectors, these devices feature both row and column contacts implemented on the anode surface. This electron-only approach circumvents problems associated with poor hole transport in CZT that normally limit the thickness and energy range of double-sided strip detectors. These devices can achieve similar performance to pixel detectors. The work includes laboratory and simulation studies aimed at developing compact, efficient, detector modules for 0.05 to 1 MeV gamma radiation measurements. The low channel count strip detector approach can significantly reduce the complexity and power requirements of the readout electronics. This is particularly important in space-based coded aperture or Compton telescope instruments requiring large area, large volume detector arrays. Such arrays will be required for NASA's Black Hole Finder Probe (BHFP) and Advanced Compton Telescope (ACT).

Keywords: CZT, strip detectors, gamma-ray

1. INTRODUCTION

We have developed two novel designs for single-sided CZT strip detectors. The first is the *orthogonal coplanar anode strip detector*. Its design, construction and performance were presented previously[1-3]. It uses both *collecting* and *non-collecting* contacts organized in rows and columns on the anode surface to perform the energy and imaging measurements. A brief description and details on the performance of the most recent prototype detector modules is provided in Section 2.

A newer approach, the *single-sided charge-sharing strip detector*, was presented in November 2003[4]. It operates on a charge-sharing principle using only *collecting* contacts organized in rows and columns on the anode surface for the energy and imaging measurements. Compact prototype detector modules employing the new approach are in the fabrication phase. A more detailed description follows in Section 3.

The advantages of either single-sided strip detector approach are as follows.
- Far fewer electronic channels than pixel detectors with similar performance. A 32-row × 32-column device requires 64 channels, one-sixteenth the number required by the equivalent size pixel detector.
- These single-sided electron only devices can be made up to 10 mm thick, 5 times thicker than double-sided strip detectors and retain full detection efficiency throughout the volume.
- All signals are on one side simplifying the design and fabrication of closely packed arrays. Double-sided strip detectors also have the requirement that electrical signal contacts must be made to the strips on both surfaces.
- The small channel count permits ac coupling of signals to the front-end electronics (FEE) thus minimizing the sensitivity to leakage current variations among signal channels and permitting consideration of a variety of already developed front-end application specific integrated circuits (ASICs).

---

[*] John.Macri@unh.edu; phone 1 603 862-2793; fax 1 603 862-3585

- Unlike double-sided strip detectors, the row and column signals of single-sided strip detectors have correlated pulse heights. This feature may simplify resolution of the ambiguity associated with multiple Compton interaction events.

2. THE ORTHOGONAL COPLANAR ANODE STRIP DETECTOR

2.1 Anode pattern and signals

Figure 1 illustrates the anode contact pattern and readout. The pattern forms an 8×8 array of 1mm unit cells or *pixels*. A cathode contact on the opposite side is not shown. Also not shown is the guard ring electrode on the anode's perimeter. The metallic contacts are shown in gray and black. The black pixel contacts are biased to collect electron carriers and interconnected in rows on the carrier substrate for readout. A signal from each interconnected pixel row provides the event trigger as well as the energy and *y* coordinate. The gray, orthogonal, non-collecting, strip column electrodes are biased between cathode and pixel row potentials. A signal from each orthogonal strip column provides the *x* and *z* coordinates. For optimum performance, this approach requires that the strip column contacts collect no charge but only register the motions of electrons as they drift toward the anode.
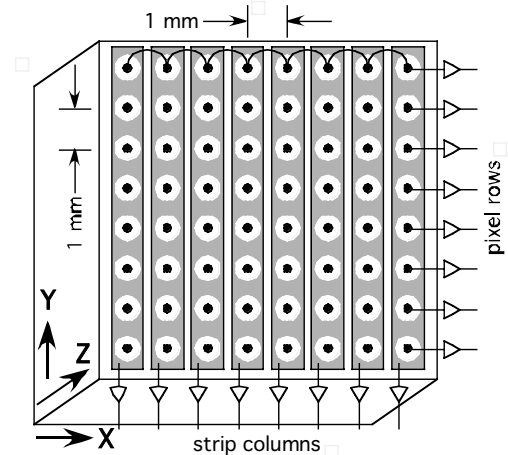

Fig. 1. Single-sided strip detector with collecting (row) and non-collecting (column) contacts on the anode surface.

Figure 2 illustrates measured and simulated detector signals (charge-sensitive preamplifier outputs) for both a pixel row and a strip column from three ^{137}Cs gamma rays interacting at different depths (z, distance from the cathode surface) in the detector. The pixel signals, rising in only the positive direction, are typical of small-pixel anodes in CZT detectors. These signals are a measure the energy deposit and identify the y-coordinate of the gamma-ray interaction. The strip signals are bipolar in nature. They have earlier initial rises than the pixel signals because they sense (in the mirror charge) the motion of the electrons before they are collected. They reach a maximum shortly before electron transit time and decrease as the electrons approach the pixel. Note that the negative residual charge remaining on the strip at the end of the event is more negative at larger z. This latter effect is due to trapped holes and can be exploited to extract the third spatial coordinate, z, the depth of interaction.

We have studied various approaches to processing the strip column signal to measure the x and z coordinates of the interaction. We have concluded that the application of a short shaping time (100-200 ns) is best for extracting the x-coordinate and that a longer shaping time, >1 µs works well for extracting the z-coordinate[3]. These approaches are relatively simple to implement. We note, however, that the faster, low noise front-end circuitry appropriate for the *x*-coordinate measurement will require more power.

All this assumes that no charge is collected on the strip electrodes. We have seen the deleterious effects of charge collection on the strip column electrodes in our earlier detector modules[4] but we have now identified a process that mitigates this problem.

2.1 Detector Modules

We have conducted a series of detector fabrication and test cycles beginning in 1999. Prototype detector modules incorporating this design with 1 mm pitch in the x and y dimensions have been fabricated using CZT material from both eV Products and Yinnel Tech, Inc. The CZT materials were processed and patterned by eV Products (Fig 3a, left). The mating ceramic
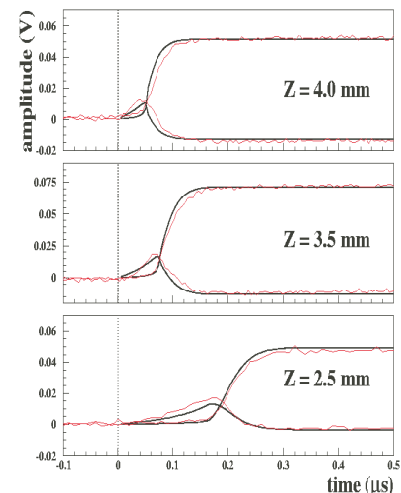
Fig. 2. Measured and simulated pixel row and strip column signals at various depths of interaction.
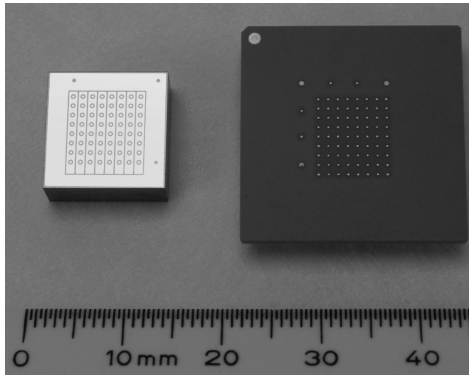
Fig. 3a. Orthogonal coplanar anode strip detector module components. Patterned CZT anode (left); mating ceramic carrier (right).
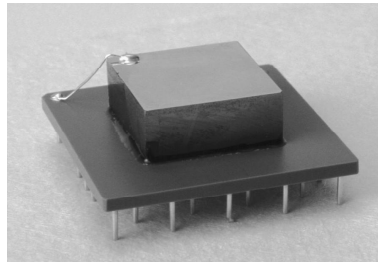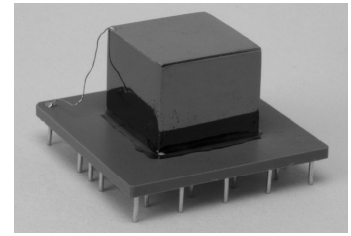
Fig. 3b. Detector module (5 mm thick).

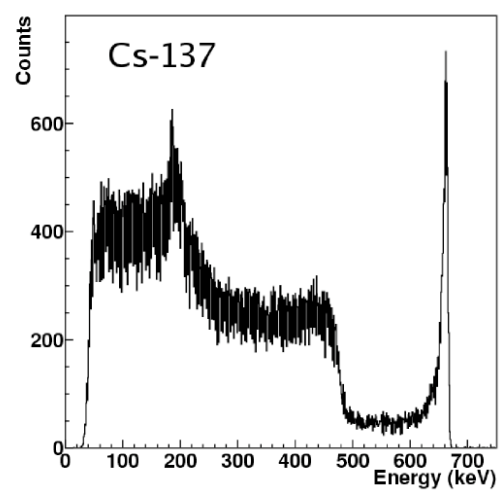Fig. 3c. Detector module (10 mm thick).
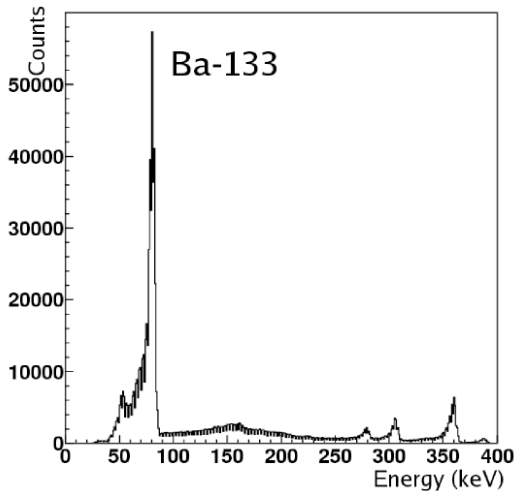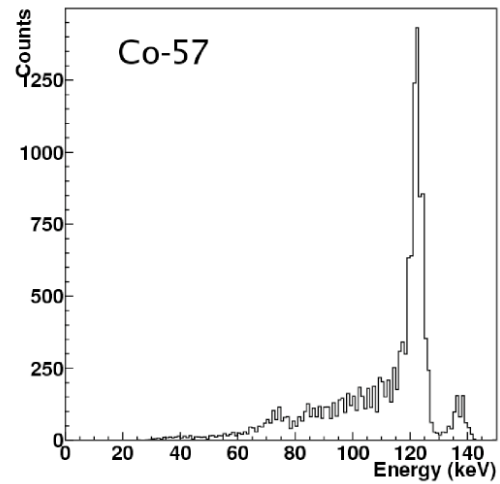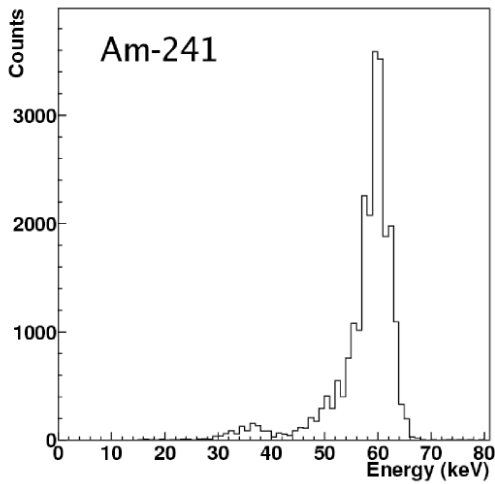
Fig. 4. Spectroscopic performance of prototype single-sided CZT strip detector. Pixel row spectra. No event selections.

substrate (Fig. 3a, right) was fabricated using low temperature cofired ceramic (LTCC) technology. Interconnection of the pixels in rows and a breakout of the detector contact elements to pins in a standard pin grid array pattern are implemented on the underside of the LTCC substrate (not shown). Two flip-chip bonding approaches have been used to

form the electrical and mechanical connections of the CZT anode to the ceramic substrate: PFC bonding by Polymer Flip-Chip Corp. and Z-bond by eV Products. In either case the result is a rugged detector module assembly (Figs. 3b, c) that involves no wire bonds to the CZT anode surface. We have performed and reported on extensive characterization testing of these module assemblies in the laboratory. The best performance has been achieved in the current year using eV Products' coplanar grid (CPG) materials and processes.

The research and development at eV Products for a line of high performance CPG spectrometers was accelerated by homeland security demands. The material selection and processing for optimal CPG detector performance requires high electron mobility and low leakage currents. This includes low surface leakage between differentially biased contacts on the anode surface. Like our single-sided strip detectors, a CPG spectrometer detector, in order to perform properly, must have both collecting and non-collecting contacts on the anode surface. The material selection and processing necessary for optimum CPG performance has been established at eV Products and employed in our most recent prototypes. A high-density electrical and mechanical bonding approach, Z-bond, also developed by eV Products, has been used here. Our prototype modules using these eV Products processes with this design has demonstrated excellent performance. The results that follow were obtained with a 5mm thick detector module fabricated this way, serial number UNH-EV-14.

The current cost for our prototypes, ~$3500 for CZT material, selection testing, patterning and bonding, however, is high. Cost is an especially important factor in large detector applications such as NASA's BHFP and ACT missions where detector requirements are specified in units of square meters and kilograms.

2.2 Spectroscopy
Spectra from flood illumination of this detector at room temperature with calibration source photons spanning a range of energies are shown in Fig. 4. Note that these are single pixel row spectra (eight 'pixels') made without any event selection or correction for interaction depth. Energy resolution (1σ) is 2.6, 3.1, 2.6, 3.1 and 3.7 at 60, 81, 122, 356 and 662 keV respectively. The electronic noise, measured with a test pulse, is equivalent to 2.1 keV.

2.3 Spectral uniformity, efficiency and CPG materials
A detailed set of measurements of the spectral uniformity and the trigger efficiency was conducted using an earlier prototype detector[4]. The detector's response was mapped across its entire imaging surface using a collimated beam of photons from a [57]Co source. We observed a clear correlation between good spectral response and full trigger efficiency. Poor and non-uniform spectral response, observed in some detector regions, correlated well with lower than expected trigger rate. The source of these problems was determined to be partial collection of the signal electrons on the 'non-collecting' strip-column electrodes. For ~25% of this detector's area, we found that up to 40% of the charge was collected on the strip column electrodes.

As mentioned above (Section 2.1), CPG spectrometer detectors, like the imaging detectors discussed here, in order to perform well, require both collecting and effective non-collecting contacts on the anode surface. With the CPG materials and processes from eV Products charge collection on the non-collecting strip column electrodes has been greatly reduced. This results in improved spectroscopic performance as shown in Section 2.2. New mapping data have been collected. We find that the spectroscopic and trigger efficiency response is uniform in 58 of the 64 'pixels' defined by the full 8 row × 8 column anode pattern of our new prototype detector. A more quantitative analysis is in progress. Meanwhile, the improved uniformity is best illustrated by the spectroscopic response of the full 64 'pixel' imaging region (Fig. 5). This [57]Co energy spectrum was formed as the composite of all eight pixel row spectra. As with the single pixel row spectra shown in section 2.2, there
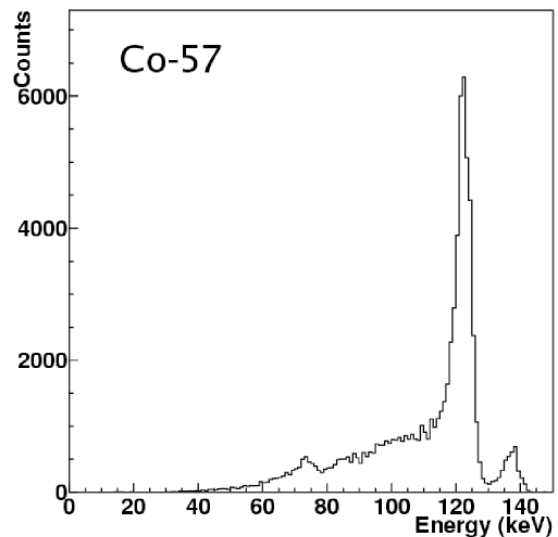

Fig. 5. Composite energy spectrum for the entire imaging region. No event selections or corrections.

are no event selections or corrections for depth of interaction. The measured energy resolution (1σ) is 2.9 keV at 122 keV.

2.4 3-d imaging

The event location capabilities are illustrated by the measured interaction locations of 122 keV photons directed in a fine beam incident on the cathode surface (Fig. 6). The 0.2 mm beam spot beam incident at ~25° from the z-axis is directed so that it enters near strip 3, pixel 1 and crosses several pixel rows and several strip columns as it passes through the 5 mm thickness of the detector. Spatial resolution is better than 1mm in all three dimensions.

3. THE SINGLE-SIDED CHARGE-SHARING STRIP DETECTOR

3.1 Detector Concept

The second concept is a *single-sided charge-sharing strip detector*. Figure 7 shows the anode pattern, the readout and two views of a 1 mm unit cell (expanded, right) to illustrate pad interconnections. Unit cells contain an array of closely packed anode contact pads in 2 groups (gray and black in this illustration). The two groups are

Fig. 6. Beam spot image, ~25° incidence. 3-d event locations. Note: cathode is at Z=0; sign of *Z* was inverted to facilitate the illustration.

identically biased for electron charge collection but are interconnected in columns or rows in the layers of the carrier substrate. A non-collecting grid electrode, biased between pixel pad and cathode potentials, provides a signal that can be used for measuring the depth of interaction, the z-coordinate. Electron charge is then shared between row and column anode pad electrodes. This is feasible when the lateral extent of the electron cloud is larger than the pitch of the anode pads. This approach takes advantage of the increasing capability of manufacturers to interconnect fine features of anode contact patterns with the carrier substrates. Interconnections, shown schematically in the figures, are implemented on the layers of the carrier substrates.

Compact prototype detector modules employing this new approach and the eV Products CPG materials and processes have been designed and are in the fabrication phase. A more detailed description follows in Section 3.5.

3.2 Advantages and disadvantages

The single-sided charge-sharing strip detector design (Fig. 7) addresses some of the limitations encountered with the earlier design (Fig. 1). The front-end electronics implementation is simplified, particularly with respect to processing the faster component of bipolar strip column signals (Fig. 2) from the earlier design. Unlike the previous design, charge collecting signals are used for the *x*- as well as the *y*-coordinate measurement. Polarities and shaping times can be the same for column and row channels. While both column and row signals will be reduced on average to half the total collected charge, the size of the non-collecting strip column signal in the previous design was only one fourth the size and required faster, and therefore noisier and higher power, processing circuitry. Surface leakage between identically biased
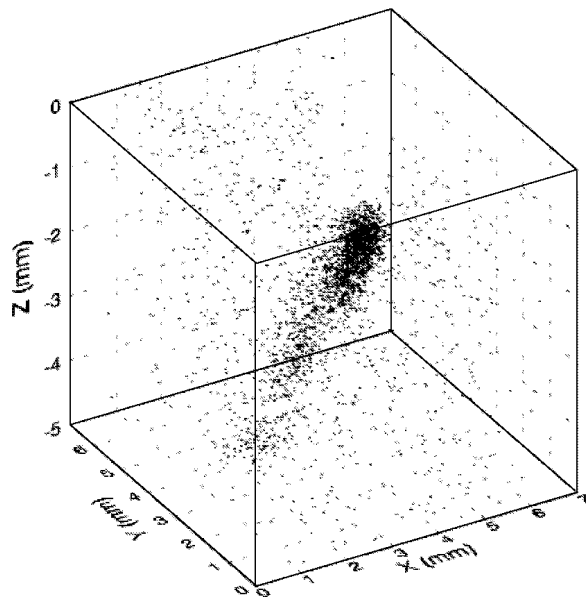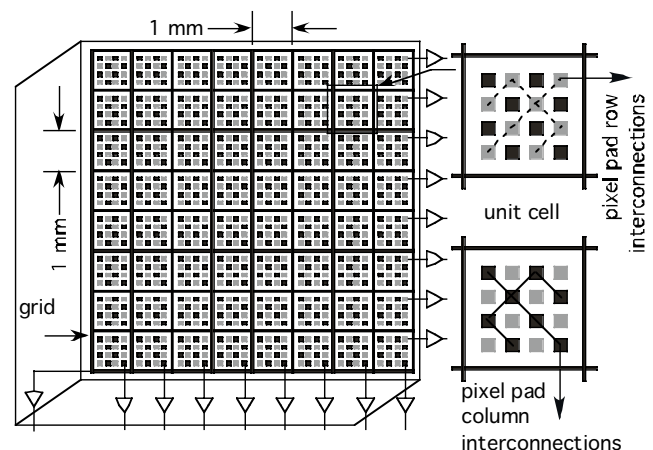

Fig. 7. Single-sided charge-sharing strip detector. Two views of a unit cell (right) show interconnections.

row and column electrodes is eliminated with this design. In addition, the large area covered by the grid electrode results in greater depth dependence of the non-collecting grid signal than was available from the individual strip column electrodes in the earlier design. (See Section 3.4.)

There are disadvantages as well. In this new design, column and row signals must be added to measure the energy. This will degrade the achievable energy resolution by a factor related to the electronic noise on each channel. We anticipate, however, that selection of the proper ASIC will minimize this effect. We also anticipate that limited charge sharing due to the small size of the electron cloud at low energies will, for some events, result in the measurement of only one of the two lateral components and will, at least for the first prototype detectors, determine the effective threshold.

3.3 Size of the charge cloud
The size of the electron cloud reaching the anode for any given interaction depends on the type of interaction, whether photoelectric or Compton, the energy deposit and the depth of interaction[5]. The range of a photoelectron in CZT is shown in Fig. 8[6]. Although these values give some idea on the size of the electron cloud, they are incomplete because secondary X-rays and electrons are not included.

To better understand the charge cloud size as a function of the photon energy, we have started more realistic Monte-Carlo simulations using GEANT (v.4.6). The preliminary result, illustrated in Fig. 9, shows the radial energy-deposit distribution from the primary photon impact point. In this simulation, Compton scattered events were excluded. We find that the electron cloud size increases abruptly from 20 keV to 30 keV due to the production of the K-shell X-rays in CZT, and that ~10% of the deposited energy lies outside the ~100 µm radius up to 150 keV. Diffusion of the charge cloud as it moves toward the anode surface will further increase the extent of the charge distribution. We calculate that charge concentrated at a point will spread to a radius of 10 µm for each mm of drift to the anode. Lower energy photons will interact nearer the cathode surface. The larger drift lengths for these events will partially compensate for the small initial size of the charge cloud.
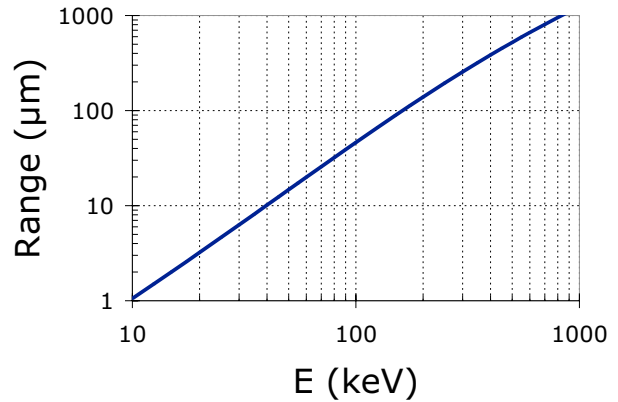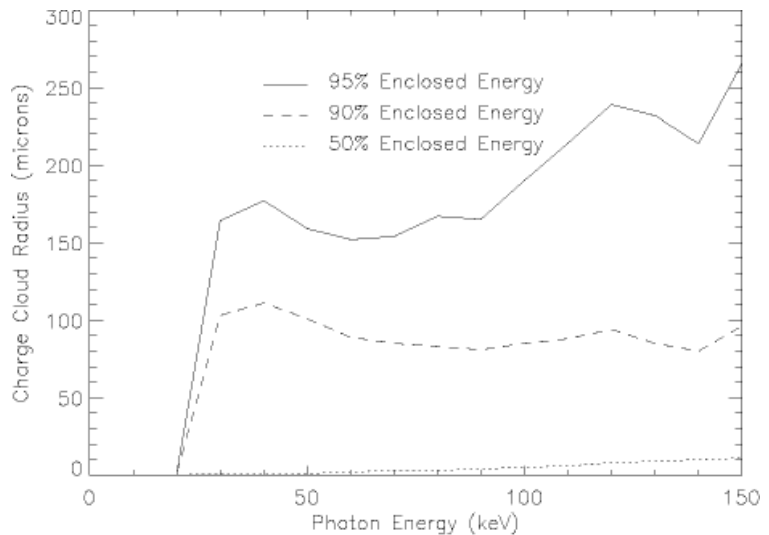

Fig. 8. Electron range in CZT.

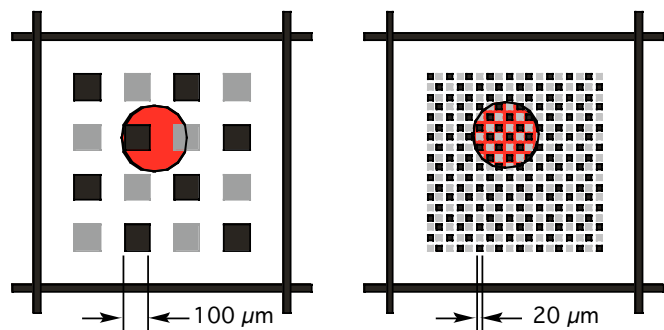Fig. 9. GEANT simulated charge cloud extent for photoelectric interactions as a function of the photon energy.

Fig. 10. Unit cells of two charge-sharing strip detectors with a 250 µm diameter charge cloud projected on the anode. Currently reasonable feature size (left); manufacturing goal (right).

The effective threshold for having sufficient shared signal to measure both the x- and y-coordinate will depend on the electronic noise and the anode pad size. A 250 μm diameter charge cloud is shown projected on two expanded unit cell anode patterns of detectors with different pad and gap sizes to illustrate how small feature size will improve the charge sharing (Fig. 10). With present manufacturing capabilities, 100 μm pads and gaps, the effective threshold will be ~150 keV. A 50 keV threshold should be possible if manufacturers can fabricate and bond detectors with 20 μm pads and gaps.

3.4 Simulations of charge-transport and signal generation

Simulations of the fields, potentials, charge transport and signal generation processes of a 10 mm thick single-sided charge-sharing strip detector (Fig. 7) were conducted at the University of Montreal. The potential across a 1 mm wide unit cell under the first millimeter of the detector is shown in Figure 11 (left). Anode pad bias is 1175 V. Grid bias is 1150 V. On the right is the weighting potential of one of the rows or columns. These plots indicate uniform fields in the bulk and that the advantages of the small pixel effect apply in this case. Simulated detector signals at various interaction depths (Fig. 12) from the charge transport and signal generation simulation are shown for one row or column (left) and for the depth-sensing grid (right). The signal pulse height is shown as a percentage of the unit charge deposited.

The simulation assumes 50:50 sharing between rows and columns of the charge signal reaching the anode surface. The simulation of row or column signals indicates little need for a depth of interaction correction of the energy measurement. The simulation of the depth sensing grid signal suggests that application of a long shaping time will be effective in establishing a measure of the depth of interaction independent of the cathode signal. Shaping times of 2 and 8 μs were simulated for the depth sensing grid signals at various interaction depths (Fig. 13). A signal-to-noise trade study is necessary to find the best solution. The ability to determine interaction depth without the cathode signal (which may be absent) is an advantage in closely packed arrays.
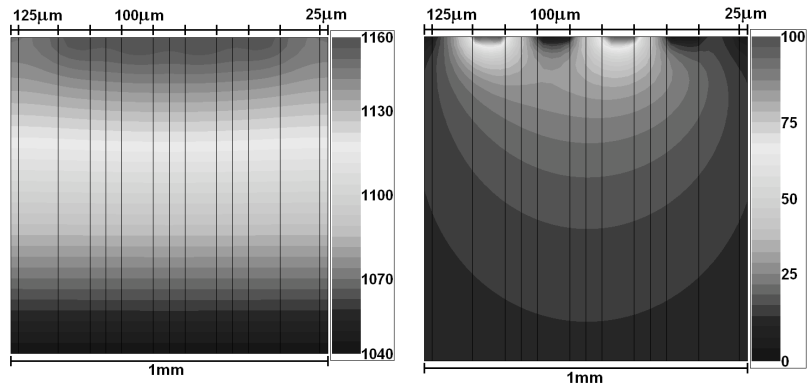

Fig 11. Simulation of a 1 mm wide unit cell for the 1st mm near the anode of a 10 mm thick detector. Potential of unit cell (left). Weighting potential of one row or column (right).
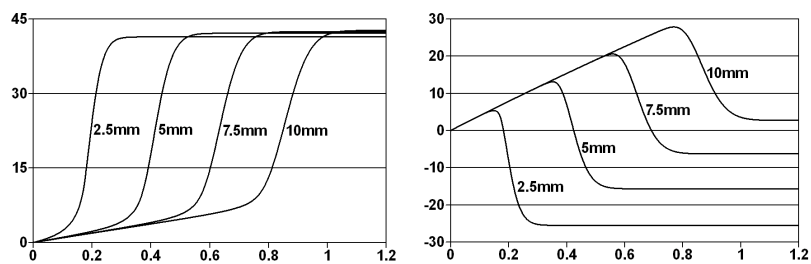

Fig. 12. Detector signals at various depths. Row or column signals (left). Depth sensing grid signals (right).
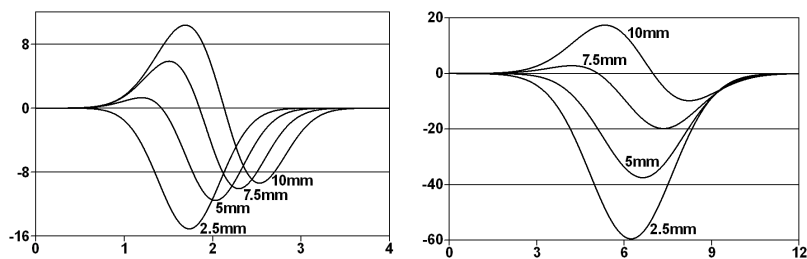

Fig. 13. Simulated depth sensing grid signals: 2 μs shaping (left) 8μs (right).

214   Proc. of SPIE Vol. 5501

3.5 Prototype Design and Construction

We have completed the prototype design and are currently awaiting delivery of our first four compact detector modules incorporating the charge-sharing strip detector design. CPG CZT materials and processing from eV Products are being employed. Figure 7 illustrates the basic anode pattern (without the guard ring). Table 1 lists the anode feature sizes for the first prototype detectors. Figure 14 shows three views to illustrate important module features and dimensions (mm). The patterned anode surface of the CZT substrate is bonded (eV Products Z-Bond) to its mating ceramic substrate. The ceramic substrate, designed for us by MillPack, Inc., is formed using Dupont Fodel layers on an alumina substrate. Multiple Fodel layers provide the mating surface contacts, the interconnection of the row contacts, the interconnection of the column contacts, a shield layer to reduce coupling between rows and columns, routing of row and column signals and biases to and from the passive component and the connector and vias to interconnect the layers.

This first prototype module design was constrained by several factors. We chose 15 × 15 × 7.5 mm detectors because CZT material of these dimensions from eV Products had already been processed and screened for CPG applications. This reduced the delivery time and the cost. The anode pad and grid widths as well as the gaps between contacts were chosen in consultation with eV Products and MillPack, the mating substrate designer. The approach was to design for the minimum feature sizes for which there was good confidence of reliable performance given present capabilities. The bonding capabilities presented the limiting factors in this case. eV Products continues to pursue improvements in its Z-bond technology with a goal of achieving 20 μm pads and gaps. The selected ceramic substrate technology, Dupont Fodel, is currently capable of 25 μm pads, vias and gaps.

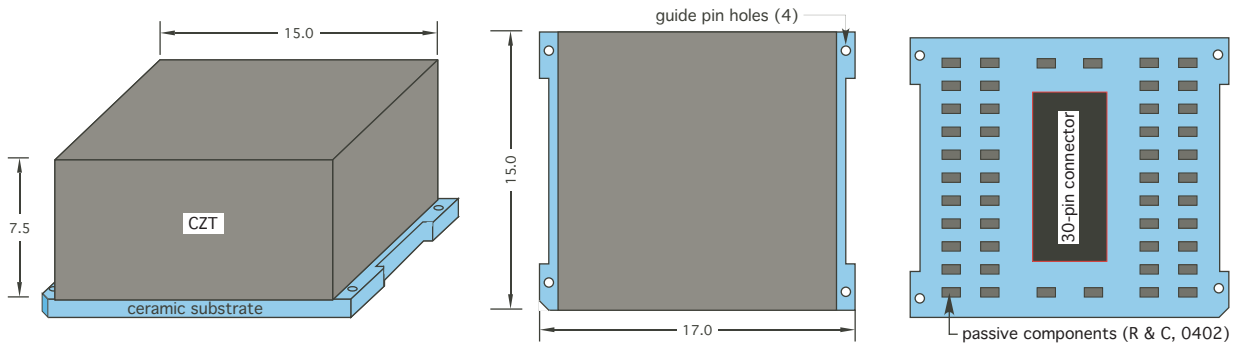| Table 1 Anode Specifications for Prototype Detectors	
columns × rows	11 × 11 (121 unit cells)
unit cell pitch	1.225 mm
pad size	125 μm × 125 μm
pad-pad gap	100 μm
grid width	125 μm
pad-grid gap	150 μm
guard ring width	250 μm
grid-guard gap	250 μm

Fig 14. Prototype detector module design. CZT (15x15x7.5 mm) bonded to ceramic substrate. Perspective, top, bottom views (l-r)

A side view (Fig 15) shows assembly of modules into an image plane. Note how the guide rails with pins on the logic board serve to align and support the modules. They also serve to conduct heat away from the detectors. We are constraining our design such that all electronics required to support a single detector module fits within the module's footprint. This design has been developed using the VA32-TA32 combination of front-end electronics application specific integrated circuits (ASIC) from Ideas. Our approach, however, is to pursue parallel development efforts for the detector module and the image plane
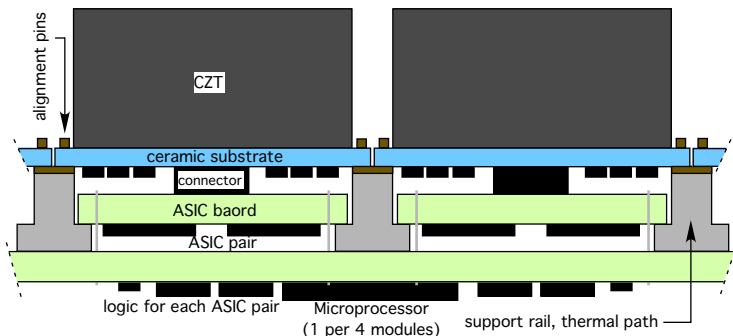

Fig 15. Image plane design. Modules plug in to an image plane assembly forming a compact array.

electronics. This allows us to consider other candidate ASICs while we continue to optimize detector design thorough our laboratory and simulation efforts.

4. MULTI-HITS

The locations of multiple Compton interactions (multi-hits) within a detector module are easily identified in pixel detectors where every pixel has its own electronic readout channel. There is, however, a potential ambiguity associated with identifying the true locations of multi-hits in strip detectors as illustrated in Fig. 16. In this example, interactions at points *A* and *B* could be interpreted as having occurred at *C* and *D*.

The data and Monte Carlo simulation analyses of UNH-eV-14 detector indicate that ~8% of all 662 keV photons register ambiguous double-hits. Unless there is some mechanism to associate the row with the column for each hit, there will be an ambiguity in the identification of the interaction sites. Independent measurements of the relative arrival time of both column and row signals can be effective unless the interactions occur at the same depth. This would come with the cost of introducing another data field for each electronics channel. If, however, the row and column pulse heights are correlated, pulse height information can be used to almost entirely eliminate this ambiguity. *A* and *B* would be identified as the true locations in this example as column,

Fig. 16. Illustration of how the correlation of row and column pulse height measurements can resolve multi-hit ambiguity.

row (2, 7) and (6, 3) record the same pulse height. The major advantage of the charge sharing strip detector design (Fig. 7) is that, once the anode feature sizes can be made small enough to achieve 50:50 row:column charge sharing, row and column pulse heights for each interaction location will be well correlated.
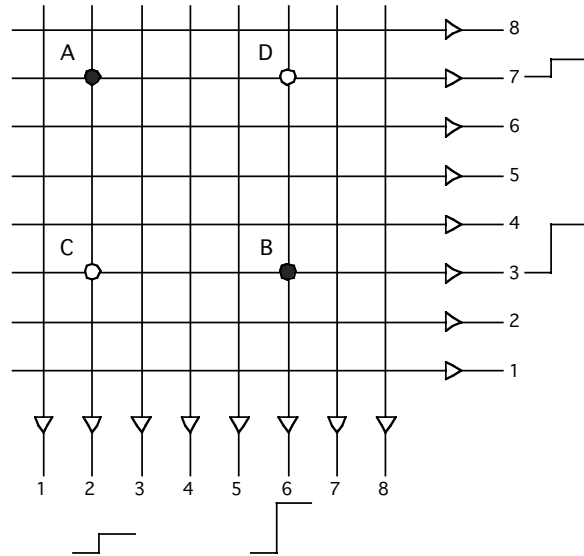
5. CONCLUSIONS AND FUTURE WORK

Our goal is to develop and demonstrate mature designs for compact, efficient, high performance CZT strip detectors for imaging and spectroscopy in the 0.05 to 1 MeV energy range and be ready to employ them in large area detector arrays when large volumes of suitable CZT material with uniform properties become available and affordable. We have developed two single-sided CZT strip detector designs. We have identified a commercially available materials selection and fabrication process that, while currently costly, is well suited to the manufacture of detectors using these designs.

A 5 mm thick prototype detector incorporating the earlier, *orthogonal coplanar anode strip detector* design, and fabricated using eV Products CPG materials and processes, exhibits significantly more uniform performance than previous devices. We have demonstrated excellent spectroscopic, imaging and detection efficiency performance with this device. The first prototype devices incorporating a new detector design approach, the *single-sided charge-sharing strip detector*, are in fabrication. We have used our charge transport and signal generation tools to help guide that design effort.

We have developed Monte Carlo simulation tools based on GEANT4 and validated these tools for spectroscopic and multi-hit response.

Future work includes the testing of the new prototype devices, compact arrays of detectors and the use of our simulation tools to help design detectors and arrays optimized for space-based astronomical observations. We will decide on one of the two single-sided strip detector approaches for further development. This will depend on the performance of the

first prototype detectors incorporating the new charge sharing design. We will also pursue single-sided strip detector designs using lower cost CZT materials.

REFERENCES

1. M. L. McConnell, J. R. Macri, J. M. Ryan, K. Larson, L.-A. Hamel, G. Bernard, C. Pomerleau, O. Tousignant, J.-C. Leroux, and V. Jordanov, "Three-dimensional imaging and detection efficiency performance of orthogonal coplanar CZT strip detectors," *SPIE*, vol. 4141, pp. 157, 2000.
2. V. T. Jordanov, J. R. Macri, J. E. Clayton, and K. A. Larson, "Multi-Electrode CZT Detector Packaging Using Polymer Flip Chip Bonding," *NIM*, vol. A458, pp. 511, 2001.
3. J. R. Macri, B. Donmez, L.-A. Hamel, M. Julien, M. McClish, M. L. McConnell, R. S. Miller, J. M. Ryan, and M. Widholm, "Readout and Performance of Thick CZT Strip Detectors with Orthogonal Coplanar Anodes," presented at IEEE Nuclear Science Symposium and Medical Imaging Conference, Norfolk, VA, 2002.
4. J. R. Macri, L.-A. Hamel, M. Julien, R. S. Miller, B. Donmez, M. L. McConnell, J. Ryan, and M. Widholm, "Single-Sided CZT Strip Detectors," presented at IEEE Nuclear Science Symposium and Medical Imaging Conference, Portland, OR USA, 2003.
5. E. Kalemci and J. L. Matteson, "Investigation of Charge Sharing Among Electrode Strips for a CdZnTe Detector," *NIMA*, vol. 478, pp. 529, 2002.
6. NIST: Physical Reference Data, ESTAR, http://www.physics.nist.gov/PhysRefData/Star/Text/ESTAR.html.